Academic Science Journal

Fabrication and Characterization of $Sn_{1-X}Cu_xO_2$ Thin Films Prepared by Chemical Spray Pyrolysis Technique

Aymen G. Hasan*, Ziad T. Khodair and Ammar A. Habeeb

Department of Physics – College of Science – University of Diyala

aimanjamhoor@gmail.com

Received: 7 August 2022 **Accepted: 12 October 2022**

DOI: https://doi.org/10.24237/ASJ.01.03.664C

Abstract

In this work, Cu NPs have been prepared by (PLA) method to ablate the Cu metallic target. The laser ablation process is done at energy by 540 and 700 mJ) at wavelengths of 1064 and 532 nm. $Sn_{1-x}Cu_xO_2$ thin film prepared by used chemical spray pyrolysis technique at x = 0.03, 0.05, 0.07 and 0.09. XRD measurements of the prepared thin films showed that thin films have a polycrystalline with a tetragonal structure, the crystallite size average of thin films increases randomly as Cu NPs ratio increased, and it was maximum (~ 30.7nm) for the $Sn_{0.93}Cu_{0.07}O_2$ thin film prepared. AFM results showed that the $Sn_{0.93}Cu_{0.07}O_2$ thin films have maximum grain size with roughness and RMS of the thin films.

The optical properties studied in the range (300- 900) nm, the transmittance increased as the wavelength increasing abuot (300-450) nm, it was found that the lesser transmittance (79%) for $Sn_{0.95}Cu_{0.05}O_2$, the energy band gap firstly is decreasing after that is increasing as copper NPs ratio increasing, as its value about (4.05-3.85) eV.

Keywords: PLA, Chemical spray pyrolysis, XRD diffraction, Optical Properties.

Academic Science Journal

تصنيع وتوصيف أغشية Sn1-XCuxO2 الرقيقة المحضرة بطريقة التحلل الكيميائي الحراري

ايمن جمهور حسن، زياد طارق خضير وعمار عايش حبيب

قسم الفيزياء – كلية العلوم – جامعة ديالى

الخلاصة

في هذا العمل تم تحضير حبيبات النحاس النانوية بطريقة الاستئصال الليزري لإزالة الهدف المعدني من النحاس. تتم عملية الاستئصال بالليزر بطاقة (540 و700 mJ) بأطوال موجية 1064 و532 nm. تم تحضير اغشية $Sn_{1-X}Cu_xO_2$ بطريقة التحلل الكيميائي الحراري بنسب (0.03 , 0.05 , 0.07 , 0.09). أظهرت قياسات حيود الاشعة السينية XRD للأغشية الرقيقة المحضرة أن الأغشية ذات تركيب رباعي متعدد التبلور ويزيد متوسط الحجم البلوري للأغشية الرقيقة بشكل عشوائي مع زيادة نسبة حبيبات النحاس النانوية، وكان الحد الأقصى (حوالي 30.7 nm) لأغشية $Sn_{0.93}Cu_{0.07}O_2$ الرقيقة. أظهرت نتائج AFM أن اغشية $Sn_{0.93}Cu_{0.07}O_2$ الرقيقة لها اعلى حجم حبيبي مع خشونة وRMS للأغشية الرقيقة. تمت دراسة الخصائص البصرية في المدى (300-900) nm حيث زادت النفاذية مع زيادة الطول الموجي 300-450 nm، ووجد أن أقل نفاذية هي (79٪) لأغشية $Sn_{0.95}Cu_{0.05}O_2$، وان فجوة الطاقة تتناقص في البداية، بعد ذلك تزداد مع زيادة نسبة حبيبات أوكسيد النحاس النانوية حيث تبلغ قيمتها حوالي (3.85-4.05) eV.

الكلمات المفتاحية: الاستئصال بالليزر النبضي، التحلل الكيميائي الحراري، حيود الاشعة السينية، الخصائص البصرية.

Introduction

Synthesis of metallic nanoparticles is very important for new applications owing to their especially optical properties compared with the bulk material. Recently, the researchers and scientists have been devoted to Cu NPs to be used in various applications such as conductive films, Nanofluids, lubrication and catalysis, the nanoparticles as well-known have a good surface to volume ratio compared with the bulk material, which enables it for catalysis applications [1, 2]. Research of Tin dioxide (SnO_2) has a dramatic interest in the wide energy gap of the semiconductor's community, due to the unique photoelectric and outstanding electricals conductions properties. As well as, doping of the Tin dioxide with metal ions is used to tailor the properties of base material, which in turn has resulted in an enhancement the performance of the device [2, 3]. This makes Tin dioxide thin films excellent candidates for

great-scale applications of gas sensors, solar cells, lithium-ion batteries, and UV photodetectors [4, 5]. The objective of the present study is to prepare Cu NPs by (PLA) method and Sn1-xCuxO2 films by using the chemical spray pyrolysis method, then study and their structural and optical properties.

Experimental Details

Pulsed laser ablation (PLA) is used to prepare colloidal Cu NPs. Before starting the ablation process, the surface of the metal target is polished with sandpaper to remove the impurities, and then it is cleaned with high-purity ethanol and then with (Distilled Water). The target (Cu 99.9% purity) is positioned at the bottom of a glass vessel and immersed in distilled water (DW). The volume of water used in all ablation operations is (5 mL) and the height of the liquid above the surface of the targets is (8 mm). Also, throughout the process, the target was shifted in many directions in order to obtain homogenous ablation without texturing effect. The target ablation main parameters were using pulsed ND-YAG laser: 1064 nm and 532 nm wavelengths of (540 and 700) mJ energies and 10 ns as a pulse time. The frequency of the laser was 1 Hz, and the number of laser pulses that operated on metal targets was (100, 200, 300, 400) pulses for each energy, In the present work, the distance between the target and the laser lens (6 cm) for the target user and the diameter of the beam of the laser on the surface of the target was 2 mm. After the ablation process was determined directly for the colloidal Cu. prepared the $Sn_{1-x}CuxO_2$ film at x = 0.03, 0.05, 0.07, and 0.09 by using a chemical spray pyrolysis technique as using Tin chloride (SnCl4.5H2O) (99.9%), then the solution is prepared by dissolving 0.1 M of (SnCl4.5H2O) in distilled water, other condition such a Distance of nozzle (30±1) cm, Spraying Rate (10 ml/min), Spraying Period (10 s), The spraying time was 10 s with 2 minutes wait between any two successive sprayings, the substrate temperature is 400 ±3°C and the Air Pressure (1.6) bar was kept constant for all films are prepared by the reaction(1). Thin films are deposited glass substrates of the dimensions (2.5 ×22.5) cm2. The thickness of the prepared films is measured by using the gravimetric technique 350 nm. Films are investigated by (Shimadzu XRD/6000) copper target (Cu-Kα/ 1.541˚A) for structural properties, Atomic Force

Microscopy (AFM) from (SPM- AA3000, USA), and the optical properties studied using UV-vis spectroscopy from (Shimadzu, UV-1800).

$$SnCl_4.5H_2O + CuCl_2.2H_2O \rightarrow Sn_xCu_{1-x}O_2 \quad \text{..... (1)}$$

Results and Discussions

Results of XRD

Fig. (1) showed the X-ray diffraction results of $Sn_{1-x}Cu_xO_2$ at x = 0.03, 0.05, 0.07 and 0.09, which is in a good agreement with (JCPDS. 00-046-1088). The highest peak occurs at 2θ~26.6o which is referred to as a plane (110) for all films which are in agreement with the ref. [6, 7], as exhibited in Table (1). The peak positions and the event of more than one diffraction which revealed that the thin films are polycrystalline with a tetragonal structure [3, 7]. The intensities of the peaks are increases as the ratio of Copper NPs increases except for the sample deposited at Sn0.95Cu0.05O2. It can be noticed that decreases with increases of Copper NPs, which is in agreement with other studies [8].

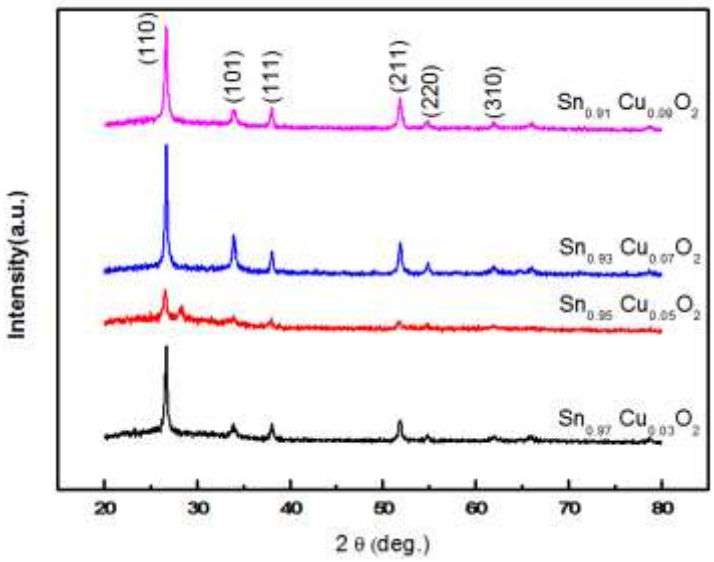

Figure1: XRD patrens of thin films

Crystalline size (D) was estimated by using Scherer's equation for (110) plane for all films [9- 12]:

$$D = \frac{K\lambda}{\beta \cos\theta} \quad \text{..... (2)}$$

Where: K is constant, λ wavelengths of X-ray incident, β: full width of half maximum for peaks, and θ angle of bragg diffraction. It's seen that average crystallite size of films increases randomly as copper NPs ratio increased, and it was maximum (~ 30.7nm) for the $Sn_{0.93}Cu_{0.07}O_2$ film prepared as shown in the Table (1). Texture coefficient (Tc) can be estimated using [12-14]:

$$T_{C(h,k,l)} = \frac{I_{(h,k,l)} / I_{\circ(h,k,l)}}{N_r^{-1} \sum I_{(h,k,l)} / I_{\circ(h,k,l)}} \quad \text{..... (3)}$$

Where the $I_{h,k,l}$ is the intensity, $I_{oh,k,l}$ is taken from the JCPDS card, N: is the number of reflections, and hkl : is the Miller indices. The Texture coefficient was used to detect the preferred directions (hkl) for the growth of the crystal in polycrystalline thin films as shown in the table1, It is clear that the Tc values >1 for all thin films, which indicates that there are numerous grains in the (110) direction [9].

Table 1: The structural properties of Sn1-xCuxO_2 thin films

SAMPLES	**2Θ (DEGREE)**	FWHM(DEGREE)	HKL	D (NM)	TC
$Sn_{0.97}Cu_{0.03}O_2$	26.6879	0.2867	(110)	28.5	1.52
$Sn_{0.95}Cu_{0.05}O_2$	26.5715	0.4522	(110)	18.1	1.28
$Sn_{0.93}Cu_{0.07}O_2$	26.7102	0.2656	(110)	30.7	1.43
$Sn_{0.91}Cu_{0.09}O_2$	26.6818	0.3117	(110)	26.2	1.45

AFM Results

The morphological examination of Sn1-xCuxO2 films at x = 0.03, 0.05, 0.07, and 0.09, was measured by using Atomic Force Microscopy (AFM), (2x2) μm2 is the size of the scanned area as shown in Fig. (2). The average roughness, root mean square (RMS) and average grain size for thin films, estimated from AFM, which are given in Table 2. The Sn0.93Cu0.07O2 thin films have a maximum grain size, roughness, and RMS of the thin film. The increase in the

average grain size is possibly produced by columnar grains growing in the structures, which is in good agreement with XRD results [7].

$Sn_{0.97}Cu_{0.03}$

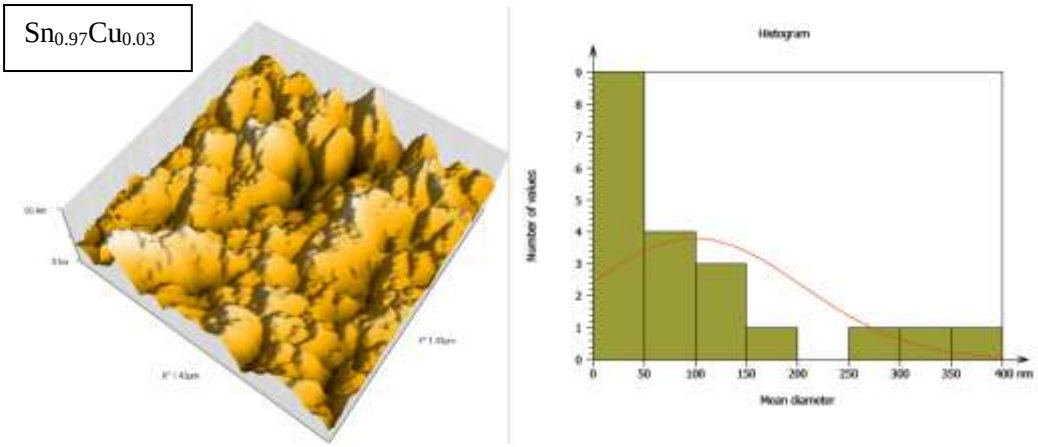

$Sn_{0.95}Cu_{0.05}O$

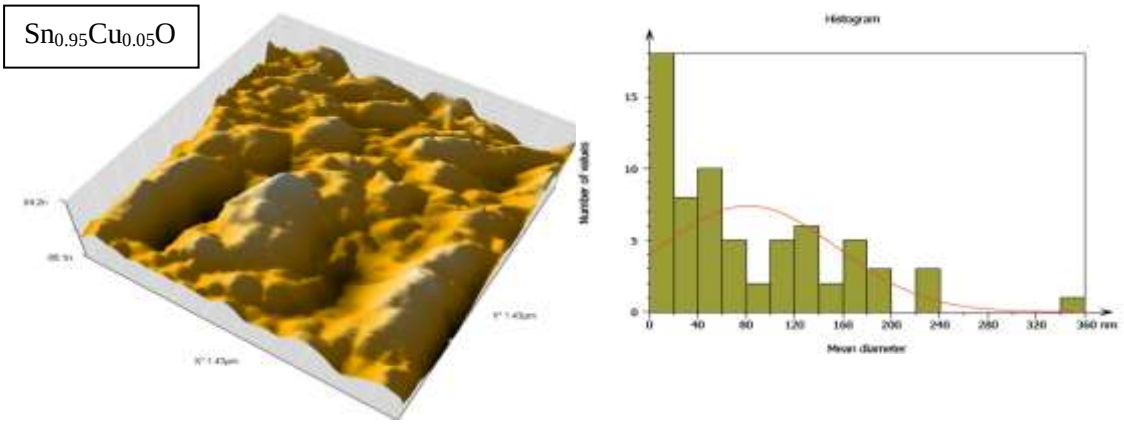

$Sn_{0.93}Cu_{0.07}$

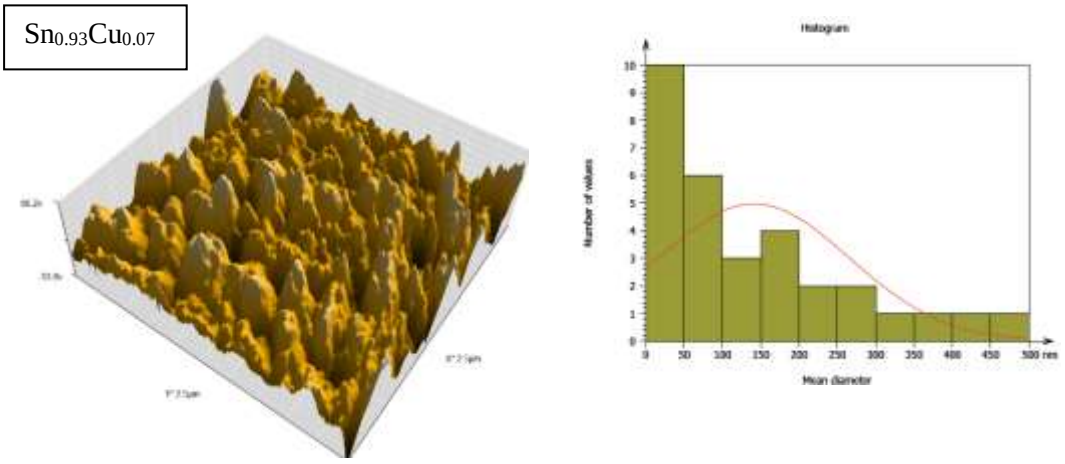

Academic Science Journal

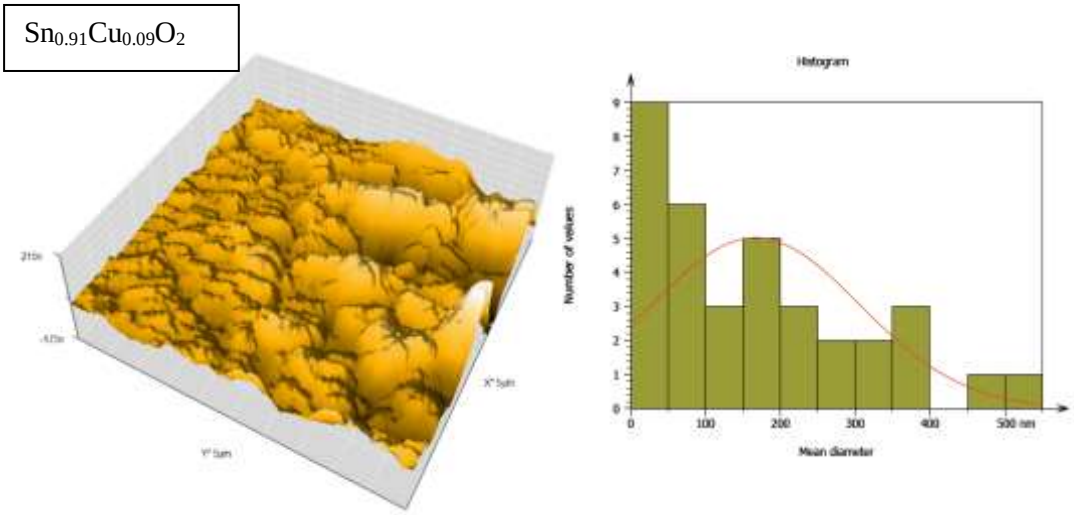

Figure 2: 3D AFM images of thin films

Table 2: AFM results of $Sn_{1-x}Cu_xO_2$ films (Root Mean Square (RMS), Surface roughness, and grain size).

SAMPLES	SURFACE ROUGHNESS (NM)	RMS (NM)	GRAIN SIZE (NM)
$Sn_{0.97}Cu_{0.03}O_2$	14.2	17.87	99.57
$Sn_{0.95}Cu_{0.05}O_2$	26.7	33.57	81.68
$Sn_{0.93}Cu_{0.07}O_2$	32.9	45.44	167.0
$Sn_{0.91}Cu_{0.09}O_2$	17.9	24.19	141.0

Optical Results

The optical properties of Sn1-xCuxO2 films with different x have been calculated by studying the transmittance and the absorbance of films within the wavelength (300 - 900) nm. Fig. (3) showed the transmittance as a function of the wavelength of films, it seen that the transmittance increased as the wavelength increased about 300-450 nm, it was found that the lesser transmittance (0.79) for Sn0.95Cu0.05O2, and the explanation for this is that the decrease leads to the formation of new localized state at the lowest of the conductions band, and these levels receive electron and create tails that work toward reducing the energy gap and thus the absorbance will increase and the transmittance will decrease [7].

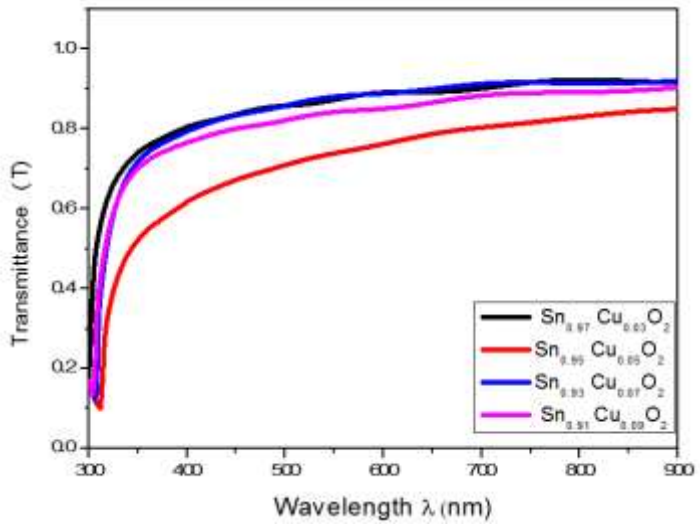

Figure 3: Transmittance against wavelength of thin films

The absorbance behavior is different for the transmittance in general, its absorbed from Fig. (4) that the absorbance decreases when the wavelength increases, about 300-550nm, and found that the higher absorbance for Sn0.95Cu0.05O2. The oxidation of Cu NPs prepared by pulsed laser ablation (PLA) also affects to blue shift in both 650 and 850 eV due to the absorption band of the film increasing at the short wavelength, which is in agreement with the References [1, 3, 7].

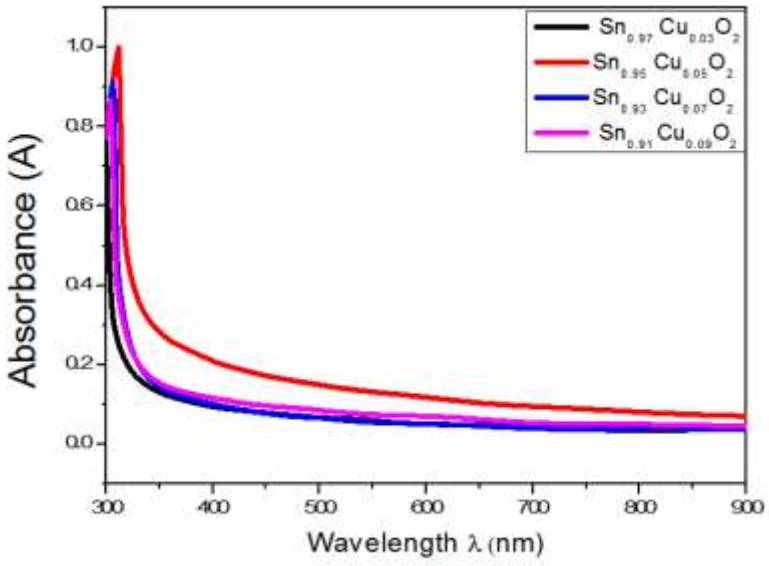

Figure 4: Absorbance against wavelength of thin films

The absorption coefficient (α) of films calculated by used [11, 12].

$$\alpha = 2.303 \frac{A}{t} \quad \text{..... (3)}$$

Where t: is the thickness of films, A: is the absorbance. Fig. (5) showed the variation of the absorption coefficient against photon energy for films, it noted that the absorption coefficient increases when the photon energy increased, the coefficient of absorption increased randomly as the copper NPs content increased and found the higher value of Sn0.95Cu0.05O2 thin film, the results indicate that the colloidal prepared at this ratio provides the highest absorption compared another. The further consequence is the oxidation of colloidal Copper NPs due to the strong reaction with the oxygen dissolved in water when prepared by PLA. This result is in high agreement with the References [1, 3].

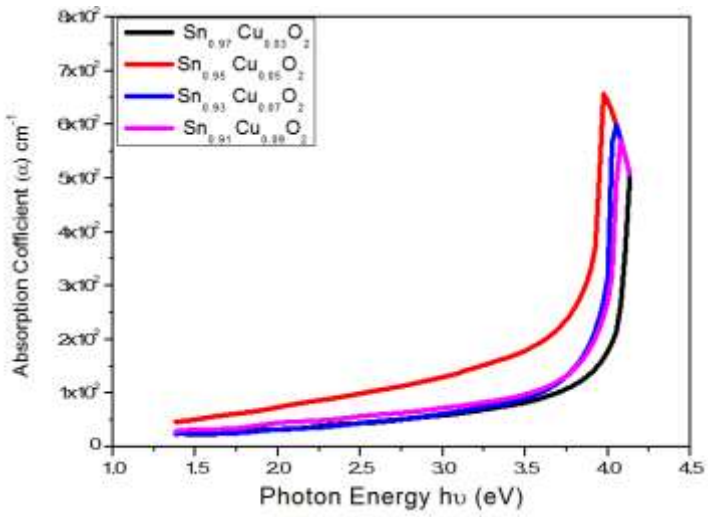

Figure 5: Absorbance coefficient against photon energy of thin films.

The energy gap of films estimated by used [15, 16]:

$$\alpha h\nu = B(h\nu - E_g)^r \quad \text{..... (4)}$$

hν: energy of the photon, B is the constant. r= 0.5 for direct transitions. The energy gap values were given by line straights to the (αhν)2 =0, as in Fig (6). It's noted that the value of the energy

gap firstly is decreasing after that is increasing as the copper NPs ratio increases as shown in table (3), the bigger value of the energy gap is due to the differences of mixed-phase thin films [3], and the crystallite size is responsible for the difference of gap [15].

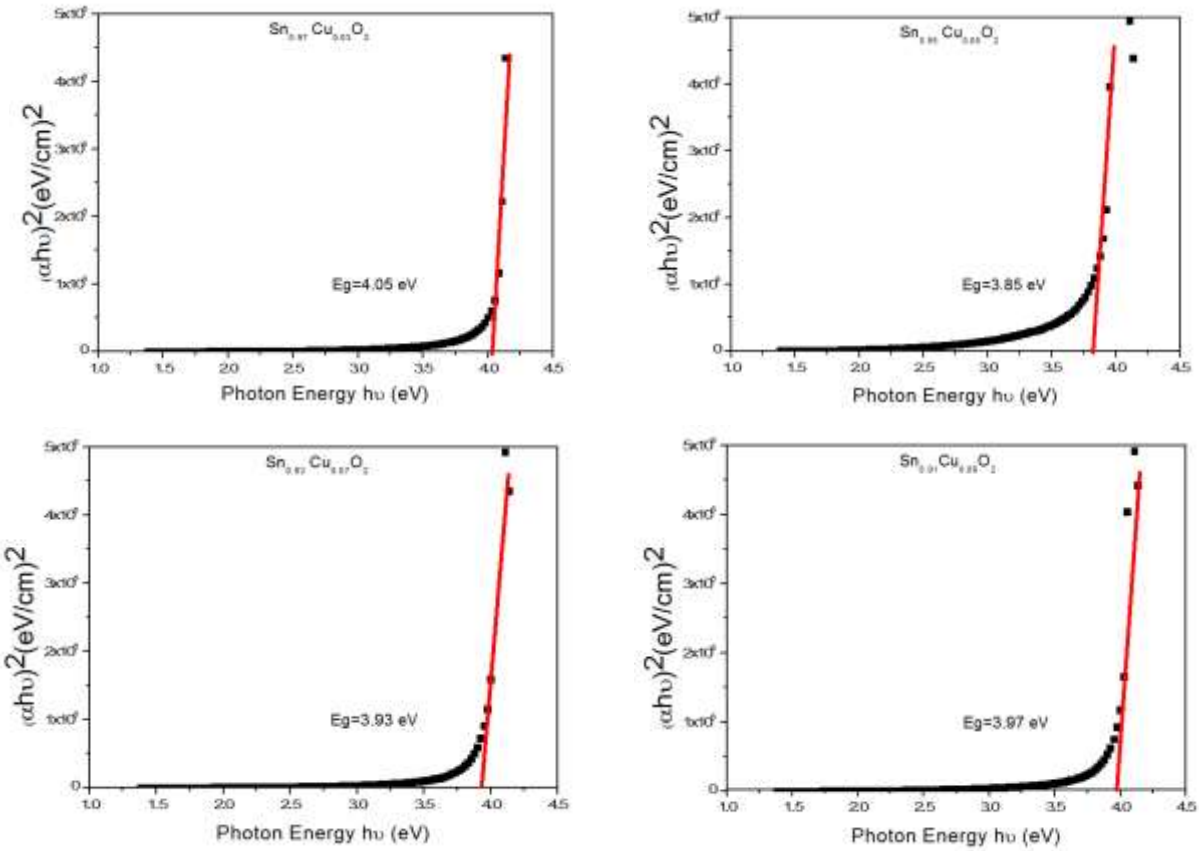

Figure 6: Energy gap for the thin films.

Table 3: The energy gap for thin films

Samples	E_g(eV)
$Sn_{0.97}Cu_{0.03}O_2$	4.05
$Sn_{0.95}Cu_{0.05}O_2$	3.85
$Sn_{0.93}Cu_{0.07}O_2$	3.93
$Sn_{0.91}Cu_{0.09}O_2$	3.97

Academic Science Journal

Extinction coefficient (K_o) is estimated by [11, 15]:

$$K_o = \frac{\alpha\lambda}{4\pi} \quad \text{..... (5)}$$

Where λ : wavelength of the photon. Fig. (7) exhibited the relation of the extinction coefficient against wavelength for all films. It observed that the coefficient of extinction decreases at short wavelengths of (300-400) nm and after that, the coefficient of extinction remains constant. The values of extinction coefficient were increased randomly with the increase of the Copper NPs ratio and found that the higher the extinction coefficient for Sn0.95Cu0.05O2 film.

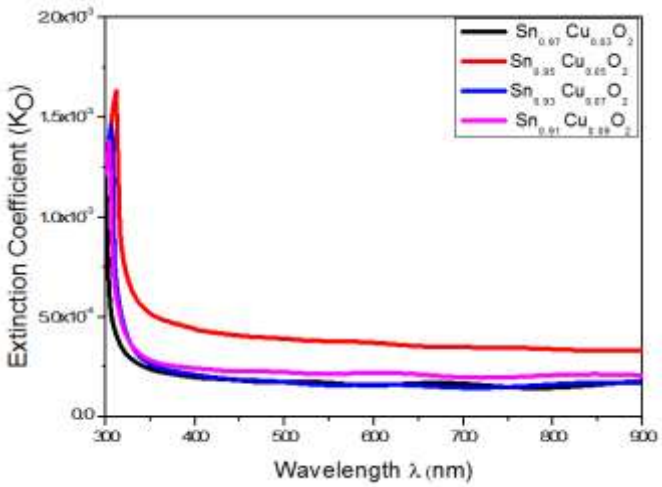

Figure 7: Extinction coefficient as a function to the wavelength

The dielectric constant of samples can be valued by [8, 13]:

$\varepsilon = \varepsilon_1 - i\varepsilon$ ..... (6)

For the determined the dielectric constant its two parts one can use the equations:

$$\varepsilon_1 = n^2 - K_o^2 \quad \text{..... (7)}$$

$\varepsilon_{12} = 2\,n\,K_O$ ..... (8)

n: refractive index, ε1, ε2: real part and imaginary part for complex dielectric constant respectively. The real and imaginary parts of the dielectric constant against photon energy for samples as shown in Fig. (8), where both the real and imaginary parts of the dielectric constant decreased when photon energy increased and the real part increased when copper NPs increased, and found that the higher value of Sn0.93Cu0.07O2 and Sn0.95Cu0.05O2 films of the real and imaginary parts respectively.

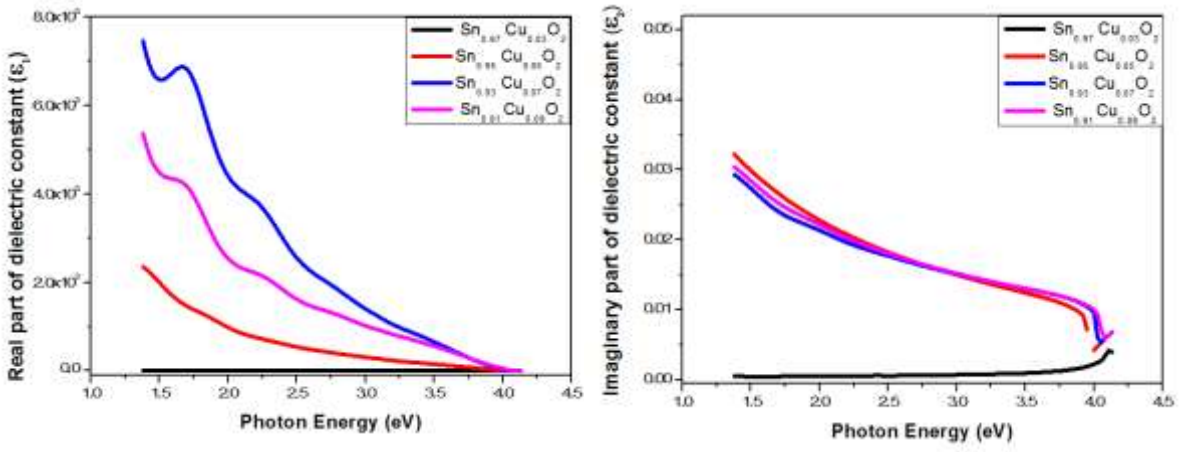

Figure 8: Real part and imaginary part of dielectric as a function to the photon energy for thin films

Conclusions

In this work, Cu nanoparticles have been prepared by PLA process to ablate Cu metallic target and the Sn1-xCuxO2 film was prepared by using chemical spray pyrolysis techniques at x = 0.03, 0.05, 0.07, and 0.09. X-ray patterns of the films explained that the films have a polycrystalline with a tetragonal structure, the maximum value of crystallite size (~ 30.7nm) for the Sn0.93Cu0.07O2 film. AFM result exhibited smooth and homogenous thin film. The optical properties studied are in the range of (300- 900) nm. The coefficient of absorption increased randomly as the copper NPs content increased. The energy band gap firstly is decreasing after that it increases as the copper NPs ratio increases, with its value of about (4.05-3.85) eV. From the study of the influence of copper NPs it has been observed that the copper NPs plays an important role in promoting the crystallinity in the films and the best sample is

Sn0.95Cu0.05O2 have minimum value of energy gab and crystallite size and can be used as window of the solar cell.

References

1. M. Mohammed, A. Diwan, S. M. Saleh, B. A. S. Salih, Kufa Journal of Engineering, 10(1), 1-11(2019)
2. Z. T. Khodair, M. A. Al-Jubbori, A. M. Shano, F. I. Sharrad, Chemical Data Collections, 28, 100414(2020)
3. G. K. Deyu, D. Muñoz-Rojas, L. Rapenne, J. L. Deschanvres, A. Klein, C. Jiménez, D. Bellet, Molecules, 24(15), 2797(2019)
4. J. S. Chen, X. W. Lou, small, 9(11), 1877-1893(2013)
5. A. Gaddari, M. Amjoud, F. Berger, J. B. Sanchez, M. Lahcini, B. Rhouta, C. Mavon, MATEC Web of Conferences, (5, 04010,EDP Sciences,(2013)
6. A. Nalin Mehta, H. Zhang, A. Dabral, O. Richard, P. Favia, H. Bender, W. Vandervorst, Journal of Microscopy, 268(3), 276-287(2017)
7. S. S. Mahmood, B. A. Hasan, Baghdad Science Journal, 16(2), (2019)
8. L. Hu, J. Yan, M. Liao, L. Wu, X. Fang, small, 7(8), 1012-1017(2011)
9. A. M. Shano, A. M. Khudhur, A. S. H. Abbas, N. A. Bakr, I. M. Ali, Synthesis, Characterization and H2S Gas Sensor Performance of Hydrothermal Prepared SnO2 Films Nanostructures. In IOP Conference Series: Earth and Environmental Science, 790(1), p. 012085). IOP Publishing(2021, June)
10. A. M. Shano, Z. S. Ali, journal of nano- and electronic physics, 12(4), 04001(5pp) (2020)
11. I. M. Ali, A. M. Shano, N. A. Bakr, Journal of Materials Science: Materials in Electronics, 29(13),11208–11214(2018)
12. I. K. Abd, A. M. Shano, E. K. Alwan, Journal of nano- and electronic physics, 14(3), 03024(4pp) (2022)
13. Z. T. Khodiar, N. F. Habubi, I. K. Abd, A. M. Shano, International Journal of Nanoelectronics & Materials, 13(3), (2020)
14. M. S. Ahmed, M. A. Iftikhar, N. A. Bakr, Journal of Nano- and Electronic Physicsthis link is disabled,11(6), 06016(2019)
15. N. F. Habubi, S. F. Oboudi, S. S. Chiad, Study of some optical properties of mixed SnO2-CuO thin films, (2012)